

Large nonlinear absorption and refraction coefficients of carbon nanotubes estimated from femtosecond z-scan measurements

N. Kamaraju, Sunil Kumar, and A. K. Sood^{a)}

Department of Physics and CULA, Indian Institute of Science, Bangalore 560012, India

Shekhar Guha

Materials Directorate, WPAFB, Dayton, Ohio 45433, USA

Srinivasan Krishnamurthy

SRI International, Menlo Park, California 94025, USA

C. N. R. Rao

CPMU, Jawaharlal Nehru Centre for Advanced Scientific Research, Bangalore 560064, India

(Received 12 October 2007; accepted 27 November 2007; published online 18 December 2007)

Nonlinear transmission of 80 and 140 fs pulsed light with 0.79 μm wavelength through single walled carbon nanotubes suspended in water containing sodium dodecyl sulfate is studied. Pulse-width independent saturation absorption and negative cubic nonlinearity are observed, respectively, in open and closed aperture z-scan experiments. The theoretical expressions derived to analyze the z-dependent transmission in the saturable limit require two photon absorption coefficient $\beta_0 \sim 1.4 \text{ cm/MW}$ and a nonlinear index $\gamma \sim -5.5 \times 10^{-11} \text{ cm}^2/\text{W}$ to fit the data. © 2007 American Institute of Physics. [DOI: 10.1063/1.2825409]

Single walled carbon nanotubes (SWCNTs) have been studied for numerous applications including third-order optical nonlinearity. These applications include nanoelectronics, gas and biosensors, field emission displays, saturable absorbers for passive optical regeneration, mode locking, and terahertz optical switching. The suspended carbon nanotubes show optical limiting due to nonlinear scattering, microplasma formation, and sublimation in the nanosecond regime.¹⁻⁵ In the femtosecond regime where heating does not play a role in the nonlinear transmission, an enormously large third-order susceptibility ($\text{Im } \chi^{(3)} \sim 10^{-6} \text{ esu}$) has been reported by resonantly exciting at the first intersubband energy levels (S_{11}) of semiconducting SWCNTs.^{6,7} The origin of this large nonlinearity is assigned to the coherence effect, rather than the incoherent or saturable absorption, because the measured nonlinearity decreased rapidly when the wavelength is changed away from the first band gap.⁶ This interpretation for the large nonlinearity is being debated.^{8,9} Other experiments^{10,11} using femtosecond pulses have reported a mixed variation with wavelength—much smaller value¹⁰ for $\text{Im } \chi^{(3)} \sim 10^{-10} \text{ esu}$ at 1.55 μm and a fairly large value¹¹ of $\sim 10^{-7} \text{ esu}$ at 1.33 μm . The origin of the nonlinearity had not been identified. In this letter, we report the results of closed aperture (CA) and open aperture (OA) z-scan measurements carried out in suspension of almost isolated SWCNTs at a wavelength of 0.79 μm (energy $\hbar\omega$ of 1.57 eV). The OA z-scan shows saturated absorption and CA z-scan reveals negative cubic nonlinear refraction. We have developed a theoretical model incorporating saturated absorption along with nonlinear absorption and refraction to derive the transmission in both the OA and CA z scans. The theoretical analysis of our results obtained with two different pulses with full width at half maximum (FWHM) of 80 and 140 fs clearly identifies two photon absorption (TPA) as the source

of nonlinearity and the TPA coefficient β is $\sim 1.4 \text{ cm/MW}$. This translates to a fairly large value of $\sim 1 \times 10^{-9} \text{ esu}$ for $\text{Im } \chi^{(3)}$ nonlinearity.

A dispersion of SWCNTs (0.4 mg) and 1% of sodium dodecyl sulfate (SDS) in water (1 ml) was sonicated for 5 h and the resultant solution was found to be well dispersed. This solution in 1 mm path length quartz cell was used in our experiments. The SWCNT sample used in our experiments is pristine and contains two diameter distributions at 1.41 and 1.58 nm as confirmed by the radial breathing Raman modes at 160 and 177.7 cm^{-1} , shown in the inset of Fig. 1.

Nonlinear transmission studies were carried out at 1.57 eV using Ti:sapphire regenerative femtosecond amplifier (Spitfire, Spectra Physics). The chosen photon energy is nearly resonant with the first interband transition energy in metallic tubes, M_{11} and off-resonant with the second interband transition energy of the semiconducting tubes S_{22} . From the absorption spectra of the dispersed nanotubes shown in Fig. 1, we infer that the absorption coefficient at this wavelength is about $5.6 \times 10^4 \text{ cm}^{-1}$. The FWHM pulse width of

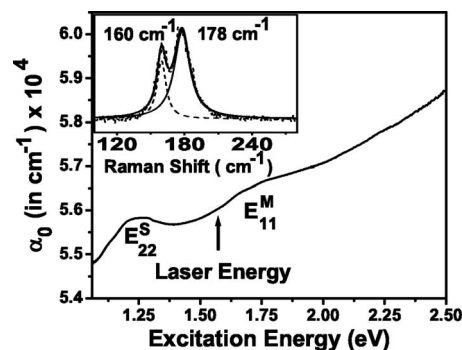


FIG. 1. Optical absorption spectrum of SDS suspended single walled carbon nanotubes in water. $E_{22}^S(E_{11}^M)$ are the second (first) interband transition energy of semiconducting (metallic) nanotubes. The inset is the Raman spectrum showing radial breathing modes.

^{a)} Author to whom correspondence should be addressed. Electronic mail: asood@physics.iisc.ernet.in.

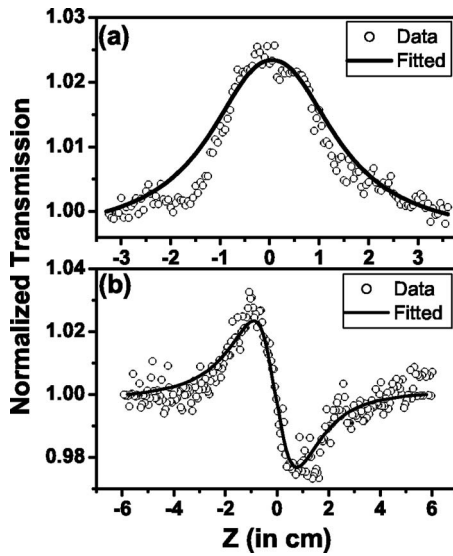


FIG. 2. Normalized transmittance data (open circles) in (a) OA z scan and (b) CA z scan ($[1 - \exp(-2r_a^2/w_0^2)] = 0.72$). Theoretical fit (solid line) is obtained with $\beta_{\text{eff}} = 1.4$ cm/MW, $I_s = 30$ GW/cm² (for OA), and 37 GW/cm² (in CA).

the amplifier output was 50 fs at a repetition rate of 1 kHz. Near the sample point, the pulse from the amplifier was found to be broadened to 80 fs. For the experiments done with 140 fs, we stretched pulse by adjusting the compressor of the amplifier. Two Si-*p-i-n* diodes [one for the signal (B) and the other for reference (A)] triggered at the electronic clock output (1 kHz) from the amplifier are used for the data acquisition and the difference between B and A was collected using a lock-in amplifier (SRS 830), averaged over 300 shots. These difference data were then converted into actual B/A signal in a personal computer. The SWCNT dispersion in 1 mm thick cuvette was translated using a motorized translation stage (XPS Motion controller, Newport) over the focal region. The intensity of input beam was varied from 150 MW/cm² to 6.2 GW/cm². In the OA z scan, all the light was collected by using a collection lens in front of the diode. The measured (and normalized) transmission data, as shown in Fig. 2(a), clearly demonstrate the saturable absorption where the transmission is enhanced at focus ($z=0$). For CA z scan, we kept an aperture of diameter 3.6 mm in front of the diode B and the measured transmission (and normalized) data, as shown in Fig. 2(b), indicate photocarrier induced reduction in the refractive index.

The procedure to calculate the transmission in z -scan experiments has been well described¹²⁻¹⁵ in the literature. For the optical limiting case, fairly accurate solutions have been used to explain the z -scan results.¹²⁻¹⁵ However, for the saturation absorption case, the solutions are obtained either qualitatively¹⁶ or in the limit where the intensity is far smaller than the saturation intensity.¹⁷ To quantify the basic mechanisms responsible for the nonlinear absorption and refraction, we accurately solve the rate equation, but modified¹⁸ for saturation absorption:

$$\frac{dI}{d\zeta} = -\frac{\alpha_0 I}{1 + I/I_s} - \beta_0 I^2 - \sigma_0 \Delta N I, \quad (1)$$

where α_0 is the one photon absorption (including intrinsic free carrier absorption) coefficient, β_0 is the fundamental TPA coefficient, and σ_0 is free carrier absorption (FCA)

cross section. I_s is the parameter that characterizes the saturation absorption. The intensity (I) at the radial position r , time t , the position ζ in the sample, and the location of the sample z is denoted as $I(z, \zeta, r, t)$. The generated photocarrier density ΔN depends on both α_0 and β_0 . In our experiment, the maximum value of I is ~ 6 GW/cm² and α_0 is $= 5.6 \times 10^4$ cm⁻¹. Even with a large value for $\beta_0 \sim 10^{-6}$ cm/W, the dominant source of carrier generation is one photon absorption. Since the carrier decay time is much longer than the pulse width τ_0 , Eq. (1) takes the form

$$\frac{dI}{d\zeta} = -\frac{\alpha_0 I}{1 + I/I_s} - \beta_{\text{eff}} I^2, \quad (2)$$

where

$$\beta_{\text{eff}} = \beta_0 + (\sigma_0 \alpha_0 \tau_0 / \hbar \omega). \quad (3)$$

The boundary condition required to solve Eq. (2) is the input intensity which is assumed to be a Gaussian and

$$I(z, 0, r, t) = I_0 \left[\frac{w_0}{w(z)} \right]^2 \exp \left[-\frac{2r^2}{w(z)^2} \right] \exp \left[-\frac{t^2}{\tau_0^2} \right], \quad (4)$$

w_0 is the beam waist at the focus, $w(z) = w_0 \sqrt{1 + (z/z_0)^2}$ is the beam radius at z , $z_0 = \pi w_0^2 / \lambda$ is the diffraction length of the beam, τ_0 is the half width at e^{-1} of the maximum of the pulse, and λ is the wavelength. The intensity at the exit side of sample, $I(z, L, r, t)$ is obtained from the analytical solution¹⁹ to Eq. (2) and integrated over all r and t to calculate the transmitted energy. The transmission in the OA z -scan experiment, $T_{\text{OA}}(z)$ is simply the ratio of transmitted energy to the incident energy. The solution to Eq. (2) depends on two parameters β_{eff} and I_s , which can be varied to fit the measured OA z -scan data. Since several sets of β_{eff} and I_s can fit the data, we will choose appropriate set that fits CA data as well.

The transmission for CA case is more complicated as it requires the phase of electric field (E) in addition to the intensity at the exit surface.^{12,14,15} The phase at $\zeta=L$ is different from that at $\zeta=0$ because of the change in refractive index, Δn , caused by light absorption. To a first order in I , the Δn is simply γI , where γ is the cubic nonlinear index.

The cubic nonlinear refraction coefficient γ in general, has contribution from the photo-generated carriers, temperature change, and bound electrons. Following the well established procedure,¹² we calculate the electric field inside the sample. For thin samples where photo-carrier generation is uniform, the change in phase from incident to exit surface is $\Delta \phi = k \gamma \int_0^L I(\zeta) d\zeta$, where k is the wavenumber and $I(\zeta)$ is the solution of Eq. (2). For a given r and t , the intensity at any ζ inside the sample is obtained analytically, fitted to polynomial series in $I(z, 0, r, t)$, and substituted for $\Delta \phi$ to get

$$I(z, \zeta) = \sum_{n=0}^6 a_n(\zeta) [I(z, 0)]^{n+1}, \quad A_n = \int_0^L a_n(\zeta) d\zeta, \quad (5)$$

$$\Delta \phi = k \gamma e^{-2r^2/w(z)^2 - t^2/\tau_0^2} \sum_{n=0}^6 A_n I_0^{n+1} \left[\frac{w_0}{w(z)} \right]^{2n+2}.$$

The electric field at the exit surface is then

$$E(z, L, r, t) = \sqrt{I(z, L, 0, 0)} e^{-[r^2/w(z)^2 + ikr^2/2R(z) + t^2/\tau_0^2 - i\Delta\phi]}, \quad (6)$$

where $R(z) = z[1 + z_0^2/z^2]$ is the radius of curvature of the wave front at z . As before,¹² $e^{i\Delta\phi}$ is expanded in infinite series and Gaussian decomposition method¹³ is used to obtain the field pattern at the aperture which is at a distance d away from the exit surface. In our calculations, we found that the convergence is achieved with first four terms in the expansion. We get normalized z -scan transmittance, $T_{CA}(z)$ by integrating $|E(z, L+d, r, t)|^2$ over all t from $-\infty$ to $+\infty$, and r from 0 to aperture radius r_a , then dividing it by $\pi^{3/2}\tau_0 w_0^2 I_0 [1 - \exp(-2r_a^2/w_0^2)]/2$.

From the difference between the normalized peak and valley transmittance in CA z -scan experiment and aperture's linear transmittance, value of γ can be calculated.¹² From our measured CA z -scan experiments [shown in Fig. 2(b)], we obtain a value of $-5.5 \times 10^{-11} \text{ cm}^2/\text{W}$ for γ . A simple calculation²⁰ using the value of $-3 \times 10^{-21} \text{ cm}^{-3}$ for (dn/dN) predicted²¹ in wide band gap semiconductors also yields a value $-3 \times 10^{-11} \text{ cm}^2/\text{W}$ for γ . However, our measured value for γ is about two orders less compared to the value predicted by Margulis and Gaiduk for SWCNTs.²² Using a value of $-5.5 \times 10^{-11} \text{ cm}^2/\text{W}$ for γ , we have then varied β_{eff} in the calculation of $T_{CA}(z)$ to fit the data. We found that both OA and CA data can be fitted simultaneously with one set of parameters, as shown by solid line in Fig. 2. With larger values of β_{eff} , a good fit to CA data could not be achieved for any value of I_s (the same is true for OA data too). Although good fit is possible with much smaller β_{eff} , the I_s required to fit CA differs considerably (by more than an order of magnitude) from that needed to fit OA data. A consistent set of parameters for $\gamma, \beta_{\text{eff}}$, and I_s , respectively, $-5.5 \times 10^{-11} \text{ cm}^2/\text{W}$, $1.4 \times 10^{-6} \text{ cm}/\text{W}$, and $30 \text{ GW}/\text{cm}^2$, fit both OA and CA data well as shown by solid lines in Fig. 2. As seen from Eq. (3), the β_{eff} has two contributions: TPA and FCA. Noting that the FCA contribution depends on the pulse width, we repeated both CA and OA z scan with FWHM of 140 fs to evaluate the relative strength of these two contributing mechanisms. We found that z -scan data with 140 fs pulse width are identical to that obtained with 80 fs pulse width. This clearly indicates that FCA cross section is extremely small and the fundamental TPA (β_0) is the dominant mechanism for nonlinear absorption. The predicted value of $1.4 \text{ cm}/\text{MW}$ for β_0 in CNTs is two to three orders of magnitude larger than that in wide band gap semiconductors at $1-2 \mu\text{m}$ wavelength. This large value of nonlinearity (both β_0 and γ) arises mainly as the consequence of the one dimensional motion of delocalized-electron cloud along the nanotube axis.^{23,24} Although the large value of β_0 at the wavelength, where α_0 is also large, makes it less useful for

optical limiting applications, the underlying mechanism responsible for β_0 could be operative even at the forbidden wavelength. With our increasing ability to tune the band gap with nanotubes' radius, CNTs offer an interesting possibility for enhanced nonlinearity in near visible to short wave infrared wavelength region.

A.K.S. thanks Department of Science and Technology, India for financial support and S.K. thanks the Indian Institute of Science for his two-month sabbatical visit.

¹P. Chen, X. Wu, X. Sun, J. Lin, W. Ji, and K. L. Tan, Phys. Rev. Lett. **82**, 2548 (1999).

²X. Liu, J. Si, B. Chang, G. Xu, Q. Yang, Z. Pan, S. Xie, and P. Ye, Appl. Phys. Lett. **74**, 164 (2000).

³S. R. Mishra, S. C. Rawat, S. C. Mehendale, K. C. Rustagi, A. K. Sood, R. Bandyopadhyay, A. Govindaraj, and C. N. R. Rao, Chem. Phys. Lett. **317**, 510 (2000).

⁴L. Vivien, D. Riehl, P. Lancon, F. Hache, and E. Anglaret, Opt. Lett. **26**, 223 (2001).

⁵X. Sun, R. Q. Yu, G. Q. Xu, T. S. A. Hor, and W. Ji, Appl. Phys. Lett. **73**, 3632 (1998).

⁶A. Maeda, S. Matsumoto, H. Kishida, T. Takenobu, Y. Iwasa, M. Shiraishi, M. Ata, and H. Okamoto Phys. Rev. Lett. **94**, 047404 (2005).

⁷Y. Sakakibara, S. Tatsuurai, H. Katura, M. Tokumoto, and Y. Achiba, Jpn. J. Appl. Phys., Part 1 **42**, 494 (2003).

⁸C.-X. Sheng and Z. V. Vardeny, Phys. Rev. Lett. **96**, 019705 (2005).

⁹H. Okamoto, S. Matsumoto, A. Maeda, Y. Kishida, Y. Iwasa, and T. Takenobu, Phys. Rev. Lett. **96**, 019706 (2006).

¹⁰Y. C. Chen, N. R. Ravavikar, L. S. Schadler, P. M. Ajayan, Y. P. Zhao, T. M. Lu, G. C. Wang, and X. C. Zhang, Appl. Phys. Lett. **81**, 975 (2002).

¹¹S. Tatsuura, M. Furuki, Y. Sato, I. Iwasa, M. Tian, and H. Mitsu, Adv. Mater. (Weinheim, Ger.) **15**, 534 (2003).

¹²M. Sheik-Bahae, A. A. Said, T. H. Wei, D. J. Hagen, and E. W. Van Stryland, IEEE J. Quantum Electron. **26**, 760 (1990).

¹³D. Wearie, B. S. Wherrett, D. A. B. Miller, and S. D. Smith, Opt. Lett. **4**, 331 (1979).

¹⁴P. B. Chapple, J. Staromlynska, J. A. Hermann, and T. J. McKay, J. Non-linear Opt. Phys. Mater. **6**, 251 (1997).

¹⁵M. Yin, H. P. Li, S. H. Tang, and W. Ji, Appl. Phys. B: Lasers Opt. **70**, 587 (2000).

¹⁶Y. Gao, X. Zhang, Y. Li, H. Liu, Y. Wang, Q. Chang, W. Jiao, and Y. Song, Opt. Commun. **251**, 429 (2005).

¹⁷L. Yang, R. Dorsinville, Q. Z. Wang, P. X. Ye, R. R. Alfano, R. Zamboni, and C. Taliani, Opt. Lett. **17**, 323 (1992).

¹⁸M. Samoc, A. Samoc, B. Luther-Davies, H. Reisch, and U. Scherf, Opt. Lett. **16**, 1295 (1998).

¹⁹I. S. Gradshteyn and I. M. Ryzhik, *Table of Integrals, Series, and Products* (Academic California, 1992), pp. 68–69.

²⁰The Δn arising from the photogenerated carriers is $[\Delta n(dn/dN)]$. Then γ is simply $(dn/dN)(\alpha_0 r_0/\hbar\omega)$.

²¹Z. G. Yu, S. Krishnamurthy, and S. Guha, J. Opt. Soc. Am. B **23**, 2356 (2006).

²²V. A. Margulis and E. A. Gaiduk, J. Opt. A, Pure Appl. Opt. **3**, 267 (2001).

²³V. Margulis and T. Sizikova, Physica B **245**, 173 (1998).

²⁴J.-S. Lauret, C. Voisin, G. Cassabois, J. Tignon, C. Delalande, Ph. Roussignol, O. Jost, and L. Capes, Appl. Phys. Lett. **85**, 3572 (2004).